Plant Physiology and Biochemistry 142 (2019) 73–83

Contents lists available at ScienceDirect

Plant Physiology and Biochemistry

journal homepage: www.elsevier.com/locate/plaphy

Research article

Zinc sulphide nanoparticle (nZnS): A novel nano-modulator for plant growth

Mala Thapa[a,b,c], Mukesh Singh[c], Chandan Kumar Ghosh[d], Prasanta Kumar Biswas[b], Abhishek Mukherjee[a,*]

[a] Biological Sciences Division, Indian Statistical Institute, Rose Villa, Giridih, 815 301, Jharkhand, India
[b] Food Technology and Biochemical Engineering, Jadavpur University, 188 Raja S.C. Mallick Road, Kolkata, 700032, India
[c] Department of Biotechnology, Haldia Institute of Technology, Haldia, 721657, West Bengal, India
[d] School of Materials Science and Nanotechnology, Jadavpur University, 188 Raja S.C. Mallick Road, Kolkata, 700032, India

ARTICLE INFO

Keywords:
Zinc sulphide nanoparticles
Vigna radiata
Antioxidant system
Uptake
Translocation
Plant nano-modulator

ABSTRACT

In spite of extraordinary properties of zinc sulphide nanoparticle (nZnS), its role on plant system is not well understood, yet. Therefore, this study was aimed to assess the uptake, translocation and effects of nZnS in mung bean (*Vigna radiata*) plant at 0, 0.1, 0.5 and 1 mg L^{-1} concentrations. In this study, nZnS was synthesized by modified reflux method and physicochemical characterizations were conducted. The effects of nZnS on mung bean plant were determined by seed germination, growth parameters, membrane integrity and ROS-antioxidant defense assays. Our results showed that nZnS treatment has significantly increased seed germination, root-shoot length, pigment content and decreased lipid peroxidation. There were increased total antioxidant activity (TAA), DPPH and flavonoid contents found in treated plants. Also, nZnS treatment did not activate oxidative stress determined by SOD, CAT, CPX, APOX and GR activities. The uptake and translocation of nZnS in mung bean plants were determined by Transmission Electron Microscope (TEM) and Scanning Electron Microscope (SEM), revelling that nZnS localized primarily in the vacuoles and chloroplasts. Besides, electron micrographs showed no alteration in cell structures between treated and control plants, further confirming that nZnS treatment has no phytotoxic effects. *In vitro* and *in vivo* studies on Zn release from nZnS were also determined using Inductively Coupled Plasma Mass Spectroscopy (ICPMS) and Energy Dispersive X-ray (EDX), which showed that the Zn release and particles uptake were concentration dependent. Overall, results of this study demonstrated the positive role of nZnS on growth and antioxidant defense responses in *V. radiata* at the experimental concentrations.

1. Introduction

Engineered Nanoparticles (ENPs) have emerged as one of the most innovative and rapidly growing fields in industries, agriculture and medicine sectors. Because of their unique physicochemical and optical properties, ENPs are expected to be biologically more active than their bulkier counterparts. Recent reports indicated that more than thousands of commercial products use ENPs (Berube et al., 2010). As plants play vital role in the transportation of ENPs in the food chain through uptake and bioaccumulation (Rico et al., 2013), understanding the effects of exposure to ENPs in plants is therefore, crucial. However, scientific investigation on uptake, accumulation and effect of ENPs in edible plants are still scarce. Few reports have so far demonstrated the effects of ENPs on plant agronomic traits like biomass production, enzyme activity, photosynthetic processes, oxidative stress, and DNA expressions. Prior work with plants has evaluated the toxicity of silica (SiO_2), zinc oxide (ZnO), nickel hydroxide ($Ni(OH)_2$), copper (Cu), cerium oxide (CeO_2), titanium dioxide (TiO_2), iron oxide (Fe_3O_4), gold (Au), silver (Ag), iron (Fe), and CdSe/ZnS quantum dot (QD) nanoparticles (NPs) on *Arabidopsis thaliana*, ryegrass, mesquite, and select edible plant species including wheat, mung bean, alfalfa, tomato, corn, and cucumber (Slomberg and Schoenfisch, 2012). Most recent reports have evidenced both positive and negative effects of ENPs in plants. For instance, López et al. (2017), showed that nZnO at 400 mg kg^{-1} reduced seed germination and root length by 40 and 47% in maize (*Zea mays*). Conversely, Awasthi et al. (2017), reported that nZnO treatment at 50 mg L^{-1} improved seed germination and plant biomass in wheat (*Triticum aestivum*). ENPs move via pore and the uptake and translocation of ENPs are shape, size and composition dependent (Zhang et al., 2015). Recent studies have been made to understand the uptake accumulation and translocation mechanism of ENPs. For instance, Wang et al. (2016), demonstrated the xylem and phloem mediated uptake,

* Corresponding author.
E-mail addresses: abhi.mukh@yahoo.com, amukh@isical.ac.in (A. Mukherjee).

https://doi.org/10.1016/j.plaphy.2019.06.031
Received 11 December 2018; Received in revised form 7 June 2019; Accepted 21 June 2019
Available online 26 June 2019

translocation and distribution of nCuO (20–40 nm) from root to shoot through the xylem and its reverse transport to root through the phloem in *Zea mays*. Overall, only a limited numbers of studies are available on uptake of ENPs by plant species that subsequently accumulate in the various cellular locations and alter different biochemical processes, to date (Pradhan et al., 2013; Ghafariyan et al., 2013; Lin and Xing, 2008; Yang et al., 2014). Therefore, detail studies to generate comprehensive pictures of ENPs interactions with edible plants at the physiological and biochemical levels are required for their safe use in agriculture.

Zinc sulphide nanoparticle (nZnS) is widely used nanomaterial among the different semiconductors (Fang et al., 2011). They are used in biological applications as tagging molecules (Jin et al., 2016), pharmaceuticals (Pathakoti et al., 2013), cosmetic and rubber industries (Bhattacharjee et al., 2013) and in paint (Womack et al., 2004). nZnS is nontoxic and more stable in nature than other semiconductors (Zaba et al., 2016). It has a wider band gap value than large sized ZnS and nZnO. Because of these properties, nZnS can be used in both biomedical and optoelectronic applications (Suyana et al., 2014). Certain properties pertaining to nZnS, like it's small size with larger band gap, good biocompatibility and easy synthesis are unique and advantageous, making its commercial use economical (Huang et al., 2006). The extensive industrial applications of nZnS aggravate the possibility of its environmental dispersion and plant uptake. While some researchers have conducted mammalian and eco-toxicity studies of nZnS, like effects on retinal pigment epithelial cells (Karthikeyan et al., 2016) and on the crustacean *Daphnia sp.* (Lin and Xing, 2008), studies of its environmental fate including its effects on plant system are generally rare, with some exceptions. For example, applications of nZnS at 15 ppm concentration in *Brassica juncea* seedlings resulted in improved growth and antioxidant levels in the treated plants (Nayan et al., 2016). In another study, internalization and translocation of polymer coated CdSe/ZnS QDs was studied in *A. thaliana*. This study reported that polymer coated CdSe/ZnS QD was not internalized by *A. thaliana* (Navarro et al., 2012). Conversely, in *Medicago sativa* cells, bioaccumulation of CdSe/ZnS QD occurred specifically in the cytoplasm and the nucleus (Santos et al., 2010).

Hence, the above information emphasise that detailed studies on the mechanism of uptake, translocation and effects of nZnS application in plants would be necessary to better understand its impact on plants. In view of the above information, the current study was conducted with the following objectives, (i) to study the role of nZnS application on plant growth and antioxidant defense, and (ii) to investigate the uptake and translocation of nZnS, and its effects on plant cell microstructure.

2. Material and methods

2.1. Synthesis and physicochemical characterization of nZnS

nZnS was synthesized by a modified reflux method (Suyana et al., 2014; Fu et al., 2012). Briefly, 50 mL of 1 M aqueous solution of zinc nitrate was refluxed under nitrogen atmosphere. 50 mL of 1 M sodium sulphide solution was added in a drop by drop fashion to the above solution and allowed to stir for 6 h at 80 °C. After stirring, a white thick precipitate thus obtained was centrifuged at 10,000 rpm for 10 min and washed several times with an excess amount of Millipore-water and ethanol to remove any un-reacted species. Finally, the synthesized product was vacuum dried to obtain nZnS.

Physicochemical characterizations of the synthesized particles were conducted by X-Ray Diffraction analysis (XRD, Cu K_α radiation, $\lambda = 1.5404$ Å, X-PERT PRO diffractometer), Field Emission Scanning Electron Microscopy (ZEISS FE-SEMs), High Resolution Transmission Electron Microscopy (HR-TEM, JEOL JEM 2100 HR with EFLS), Fourier Transforms Infrared Spectra (FTIR, JASCO FTIR-6300), Photoluminescence (Perkin-Elmer LS55), Ultra-visible spectroscopy (UV-3600 series, Shimadzu), Dynamic light scattering (DLS) and Zeta potential (Malvern zetasizer).

2.2. Role of nZnS application on plant growth and antioxidant defense

2.2.1. Preparation of nZnS suspensions

Effects of nZnS on plants were studied using three different concentrations viz: 0.1, 0.5 and 1 mg L^{-1}. The choice of treatment concentrations was based on previous studies like Pradhan et al. (2013), Ghafariyan et al. (2013), and Mahajan et al. (2011), which reported the bioavailability of ENPs at low concentrations (few ppm). The nZnS suspensions were prepared by sonicating nZnS powder in Millipore-water at 25 °C for 1 h. Freshly, prepared suspensions were used each time for the treatments.

2.2.2. Plant material

Effects of nZnS application on plants were studied on mung bean seedlings (*Vigna radiata*). Mung bean seeds were purchased from Berhampur Pulse and Oil Research Centre, West Bengal, India and used as experimental material. Seeds were surface sterilized using 5% sodium hypochlorite solution (w/v) for 10 min followed by thorough and repeated washing by deionized water before experimental treatments.

2.2.3. Germination test and seedling growth condition

Surface sterilized seeds were imbibed with different experimental doses of nZnS (0, 0.1, 0.5 and 1 mg L^{-1}) and kept in dark for 4 h. After that, treated seeds (n = 100) were kept in the Petridishes with filter paper moist with respective treatment solutions, for 24 h in dark at 28 °C. After 24 h, number of seeds that has developed a primary root of at least 1 mm long was counted and germination percentage was calculated according to Singh et al. (2013). The experiment was conducted with five replications.

For further experiments, germinated seeds were placed individually in square glass-plates (14·14 cm) lined by filter paper, moist with different treatment solutions (0, 0.1, 0.5 and 1 mg L^{-1}). The glass plates containing plantlets were then dipped into respective treatment doses (Saha et al., 2012) and monitored for next 10 days. The plants were watered regularly so that only the roots were submerged in the suspensions. The experiment was conducted in a completely randomized design (CRD); 5 replicates were used for each experiments and each replicate comprised a single glass plate containing 15 plantlets. Equal space was maintained between the plantlets to avoid competition among them. Plants were grown in a growth cabinet (GC-300, Lab companion) with 14 h photoperiod, 28 °C; night temperature of 20 °C and RH 40–60%, light intensity was 440 μmol m^{-2} s^{-1}.

2.2.4. Morphological parameters

The effects of nZnS on growth parameters were studied in terms of root-shoot length, fresh-dry weights of the plant, and rootlet numbers per plant.

After 10 days, roots were rinsed with deionised water and plants were separated into roots and shoots, and their length, rootlet numbers and fresh weights were determined. Dry weights were recorded by drying the plants at 80 °C for 24 h.

2.2.5. Estimation of photosynthetic pigment content

Chlorophyll was extracted using buffered aqueous 80% acetone (pH 7.8) and was estimated by Arnon's formula (Arnon, 1949). Carotenoid content was estimated following Davis et al. (2003). Carotene and xanthophyll were measured by utilizing the values of absorbance at 425 nm and 450 nm respectively.

2.2.6. H_2O_2 generation, lipid peroxidation, proline content, electrolyte leakage and total protein content

The H_2O_2 content was analyzed according to Sinha (1972) protocol. Thiobarbituric acid (TBA) test was used to measure the Malondialdehyde content (MDA), the end product of lipid peroxidation (Hodges et al., 1999). Proline content was measured following Bates et al. (1973), method. Electrolyte leakage was determined according to

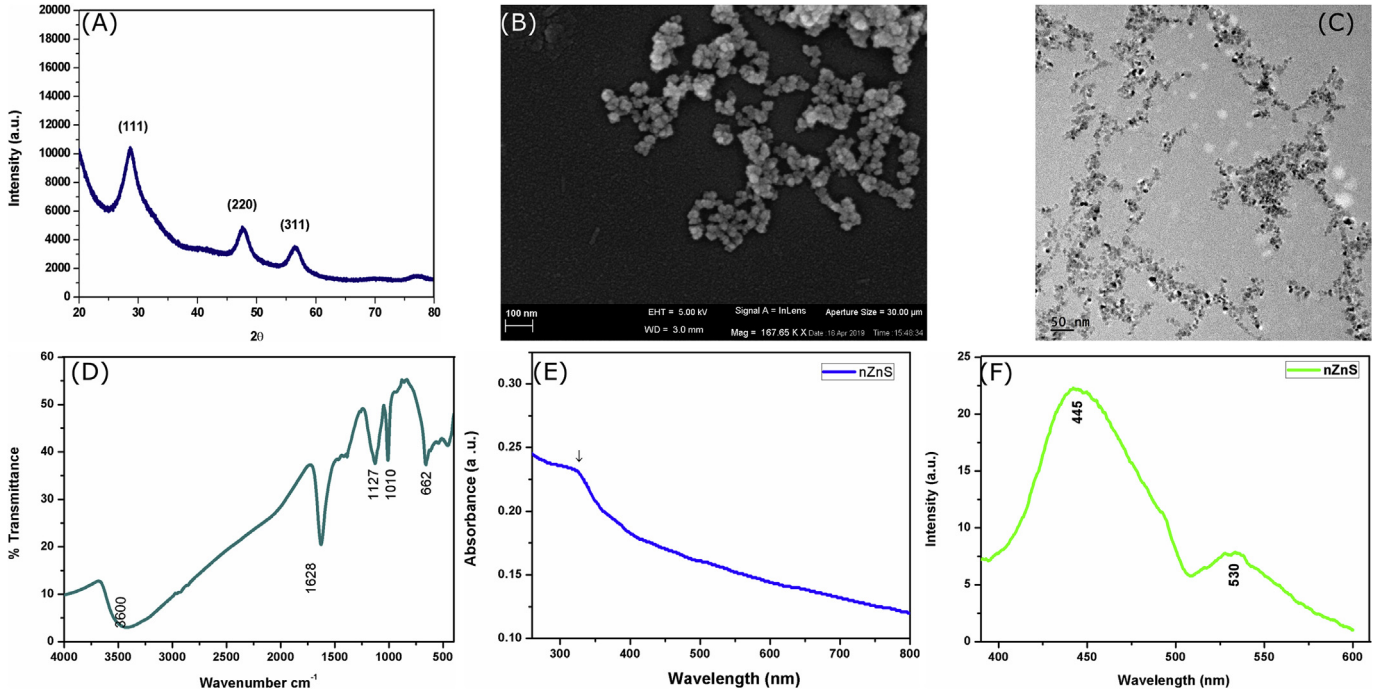

Fig. 1. (a) XRD pattern, (b) FE-SEM image, (c) FE-TEM image (d) FTIR (e) UV-spectroscopy and (f) PL spectra of synthesized nZnS.

Lutts et al. (1996), method. Total protein content was determined according to Lowry et al. (1951) and enzyme activity was expressed in terms of change in OD at 420 nm min^{-1} mg^{-1} protein.

2.2.7. Antioxidant defenses; phenol, flavonoids, total antioxidants and radical scavenging activity using DPPH

Phenol content was determined by the modified Folin-Ciocalteao method (Alhakmani et al., 2013). Flavonoids content was measured qualitatively following Ebrahimzadeh et al. (2010). Total antioxidant activities (TAA) were determined according to Prieto et al. (1999). DPPH radical scavenging activity was measured according to Blois (1958).

2.2.8. Enzyme assays

For the enzyme studies, plant material was extracted in 0.1 M phosphate buffer (pH 7) at 4 °C. Then the extract was centrifuged for 25 min at 10,000 g, at temperature 4 °C. The supernatant was used for enzymatic assays; superoxide dismutase (Giannopolitis and Ries, 1977), catalase (Chance and Maehly, 1955), peroxidase (Thurman et al., 1972), glutathione reductase (Foyer and Halliwell, 1976) and ascorbate peroxidase (Nakano and Asada, 1981).

2.3. Uptake and translocation of nZnS, and its effects on plant cell microstructure

2.3.1. SEM and TEM study

For SEM, 10 days old fresh mung bean seedlings (control and treated) were thoroughly washed with deionized water. Roots and leaves were cut in thin transverse sections (T.S.) and fixed with 2% glutaraldehyde solution at 4 °C for 2 h, followed by postfixing the samples for 2 h with 1% osmium tetroxide solution. The samples were then dehydrated with graded ethanol. Then the roots and leaves sections were coated with platinum for 60 s (ca. 1 nm platinum layer) by using a Sputter Coater and then observed under SEM (JEOL JSM-7600F, with Energy Dispersive X-ray, EDX). For TEM, 1% paraformaldehyde (PF) along with 3% glutaraldehyde was used for fixing following standard procedure (LIN, 2005). Then the samples were cut in T.S. using a microtome and observed under TEM, (Tecnai, G 20, FEI).

2.3.2. Zn release study by ICPMS

Zn release from nZnS was monitored by using Inductively Coupled Plasma Mass Spectroscopy (ICPMS, ELAN DRC-e, Perkin Elmer) at pH 7. For *in vitro* study, 100 mL of nZnS solution in Milli-Q water of treatment concentration (0.1, 0.5, and 1 mg L^{-1}) was allowed to stir for 24 h. After 24 h of stirring the supernatant was collected by centrifugation at 14,000 rpm for about 20 min. Finally the suspension were digested with ultrapure HNO_3 using standard methods (Pradhan et al., 2013), and then subjected to ICPMS using a Zn standard solution. For *in vivo* ICPMS measurement, after 10 days of treatment plants were harvested, thoroughly washed with tap water followed by rinsing with deionized water, air-dried, weighed, divided into two parts (roots and leaves), and sieved. Then the sieved plant materials were digested in a microwave accelerated reaction system using a mixture of plasma pure HNO_3 and H_2O_2 (1:4) and analyzed for Zn content.

2.4. Statistical analysis

The data were expressed as mean ± standard deviation of five replicates. Statistical differences among treatments were determined using one-way analysis of variance (ANOVA) followed by Tukey's test at a significance level of 0.05.

3. Result and discussion

3.1. Physicochemical characterization of nZnS

The XRD pattern confirmed crystalline structure of synthesized nZnS. Three characteristic peaks were obtained with 2θ = 28.5°, 47.7° and 56.5°, indexing (111), (220), and (311) diffraction planes of nZnS (JCPDS card no. 05–0566); with cubic blend structure (Fig. 1a). Additional peaks of impurities were absent signifying nZnS phase purity. Meanwhile, the morphology of synthesized nZnS was detected using FE-SEM, showed its nearly spherical morphology, which were homogenous in shape, (Fig. 1b). HR-TEM image of synthesized nZnS justified the same spherical morphology. The sizes of the particles were ≤ 20 nm with an average diameter of 13.3 ± 0.3 nm, (Fig. 1c). The surface properties of nZnS were further analysed by the FTIR spectra. The

surface of nZnS consisted of mainly three deep set (1127, 1010 and 662 cm^{-1}) in the transmittance spectra. The peaks at 1121 and 1001 cm^{-1} attributed to S-O stretching and the one that appeared at 660 cm^{-1} was assigned to the nZnS (Pathak et al., 2013). Also, the peaks cantered at 3400-3600 cm^{-1} (OH-stretching) because of some absorbed moisture and at 1628 cm^{-1} is due to the C=O stretching modes arising from the absorption of atmospheric CO_2 on the surface of the nanocrystals, (Fig. 1d). In addition, a small but negative zeta potential of −4.84 mV at 25 °C (pH 7) was observed which corroborated its surface functionality and stability. The UV absorption spectra revealed a characteristic hump shaped curve of nZnS, with a strong absorption at 324 nm (band gap = 3.82eV, Fig. 1e). The luminescence spectrum of nZnS upon excitation at 270 nm is presented in Fig. 1f. A luminescence peak at 445 nm was attributed to the defect state (S^{-2}) related to the emission from the nZnS host, while the peak at 530 nm was assigned to the S vacancy.

Prior to application the stability of nZnS was also checked with the aid of their hydrodynamic radius measurements which were found to be around 100 nm [Supporting Information, Fig. S1]. The hydrodynamic radius justified that nZnS produced a stable dispersion, and the size of the dispersed particles remains well within the nano size range that could be used under hydroponic condition.

3.2. Role of nZnS application on plant growth and antioxidant defense

3.2.1. Seed germination and plant growth morphology

In the present study, seed germination and plant growth was positively altered by nZnS treatment. A significant ($F = 5.74$ and $p = 0.007$) increase in germination percentage of treated seeds over control was observed. The highest percentage of seed germination was 98%, occurred at 0.1 mg L^{-1} nZnS concentration. The treated seeds did not show any visible signs of toxicity such as stunting, wilting, etc.

The entries of ENPs into seeds are a tough task compared to plant cell walls and membranes due to its thick seed coat. The water transport pathways are responsible for the translocation of ENPs within seeds and plants (Thurman et al., 1972), suggesting the penetration capability of nZnS through seed coat via water transports system that promoted the germination. Also, it was reported that large size aggregates of ENPs had induced toxicity in the seeds by blocking the ion and water channels or apoplastic pathway (Asli and Neumann, 2009). However, as no phytotoxic symptoms were observed in nZnS treated seeds, it can be concluded that the aggregates of nZnS did not induce any physical toxicity in mung bean seeds. Previously, Siddiqui et al., 2014, reported an enhanced seed germination of *Lycopersicon esculentum at* 8 g L^{-1} concentration of $nSiO_2$ (Siddiqui and Al-Whaibi, 2014). Similarly, Almutairi (2016), reported an enhanced germination of seeds in *Lycopersicon esculentum* at low concentration of SiNPs. Our result was in correspondence with the earlier report and suggested that the use of low concentrations of nZnS and minimal uptake by seeds could be one of the reasons to have enhanced seed germination [Supporting Information, Fig. S2].

Growth profile of the treated plants was also measured in terms of root-shoot lengths, fresh-dry weights and rootlet numbers. In our study no phytotoxic symptoms were observed either in leaf or in root at any treatment concentrations of nZnS. All treated plants were healthy and significant enhancement in growth profile was observed after 10 days of treatment (Fig. 2A). As summarized in Table 1, 0.1 mg L^{-1} concentration of nZnS was found to be the most effective among all the applied dosages of nZnS. At this dose, nZnS significantly increased root and shoot length of mung bean plants by 46.84% and 31.38%, respectively over control. Besides, fresh and dry weights (wt.) of nZnS treated plants at 0.1 mg L^{-1} concentration were also increased by 68.59% and 37.67%, respectively. Rootlet number of nZnS treated plants at 0.1 mg L^{-1} concentration was also increased by 31.51%. Previously, Suriyaprabha et al, 2012, showed significant effects of SiNPs on *Zea mays* in hydroponic medium and found that germination rate and growth percentage were enhanced (Suriyaprabha et al., 2012). The direct uptake of ENPs by seeds was improved in a hydroponic incubation that rendered potential barriers for plants and hence beneficial results were obtained. According to Rawat et al. (2019), at optimal concentration and medium term exposure ENPs can be used as a plant growth promoter or fertilizer. Our results were corroborated previous findings and suggested the positive effect of nZnS on growth of mung bean plants that can be used as plant-nanomodulator in future.

3.2.2. Pigments content

Photosynthesis is a sensitive physiological process. Its efficiency decreases under stress conditions. To determine the effects of nZnS application on photosynthesis, we measured the pigment content of the nZnS treated plants. The results showed that, plants exposed to nZnS had significantly higher pigment content than control. Among all the treatment concentrations, highest chlorophyll content was observed at 0.1 mg L^{-1} concentration, where chlorophyll *a* (Chl a) was 84.4% and chlorophyll *b* (Chl b) was 85.7% higher than those of control (Chl a; $F = 24.556$, $p \leq 0.001$ and Chl b; $F = 12.266$, $p \leq 0.001$, Fig. 2B). Similarly, highest carotenoids content was also found in plants exposed to 0.1 mg L^{-1} nZnS treatment, where carotene was 88.6% and xanthophylls was 86% higher than control (carotene; $F = 65.440$, $p \leq 0.001$ and xanthophyll; $F = 37.012$, $p \leq 0.001$, Fig. 2B).

Previously, Mukherjee et al. (2014), demonstrated that nZnO at 125, 250 and 500 mg L^{-1}, reduced chlorophyll level in peas (*Pisum sativum*). In contrast, Ghafariyan et al. (2013), reported that in *Glycine max* chlorophyll level was significantly increased by FeNP treatment at 30–60 ppm concentration. In our study, significant enhancements in both Chl a and b contents in nZnS treated plants over control were observed. As Chl a molecule participates in the photochemical reaction and Chl b on the other hand is accessory pigments that act indirectly in photosynthesis by transferring energy to Chl a, our results suggested that nZnS treatment could enhance plant photosynthate production. Also, as Chl a molecules are directly associated with carbohydrate production, responsible for better growth in vascular plants (Nayan et al., 2016), the growth increment observed in nZnS treated plants could be via increased carbohydrate production.

Carotenoids are the light harvesting accessory pigments that absorb light energy and transfer to the chlorophyll molecules and play an important role in protecting the chlorophyll from oxidative damage. Therefore, increased carotenoid contents by nZnS treatment would improve the activity of Electron Transport Chain (ETC) and provide protection from oxidative damage in plants (Pradhan et al., 2013). Overall, enhanced photosynthetic pigment contents in the treated plants suggested that nZnS could play an important role in augmenting plant's photosynthesis.

3.2.3. H_2O_2 generation, lipid peroxidation, proline, electrolyte leakage and total protein; in light of ROS generation

ENPs generate ROS, which induce lipid peroxidation, membrane leakage etc. and could cause oxidative stress in plants. To test the effects of nZnS on membrane integrity and oxidative stress; H_2O_2 generation, lipid peroxidation, electrolyte leakage, proline and protein content were measured in nZnS treated and control plants. H_2O_2 plays a vital role in plant defense system. At optimal concentrations (4 μmol m^{-2} s^{-1}), it acts as a signaling molecule involved in signaling and triggering cellular growth, whereas at relatively higher concentrations (10 μmol m^{-2} s^{-1}) it triggers loss of enzymes activity, induces oxidative stress and programmed cell death (Nakano and Asada, 1981). In our study, none of the nZnS treatment doses resulted in any significant accumulation of H_2O_2 as compared to the control (Fig. 3a). This result indicated that at the tested concentrations, nZnS did not cause any cellular stress. The recorded H_2O_2 concentrations in treated plants are in the optimal range (1.6–3.15 μM gm^{-1} fresh weight) indicating that it might be involved in the activation of cellular growth and antioxidant responses.

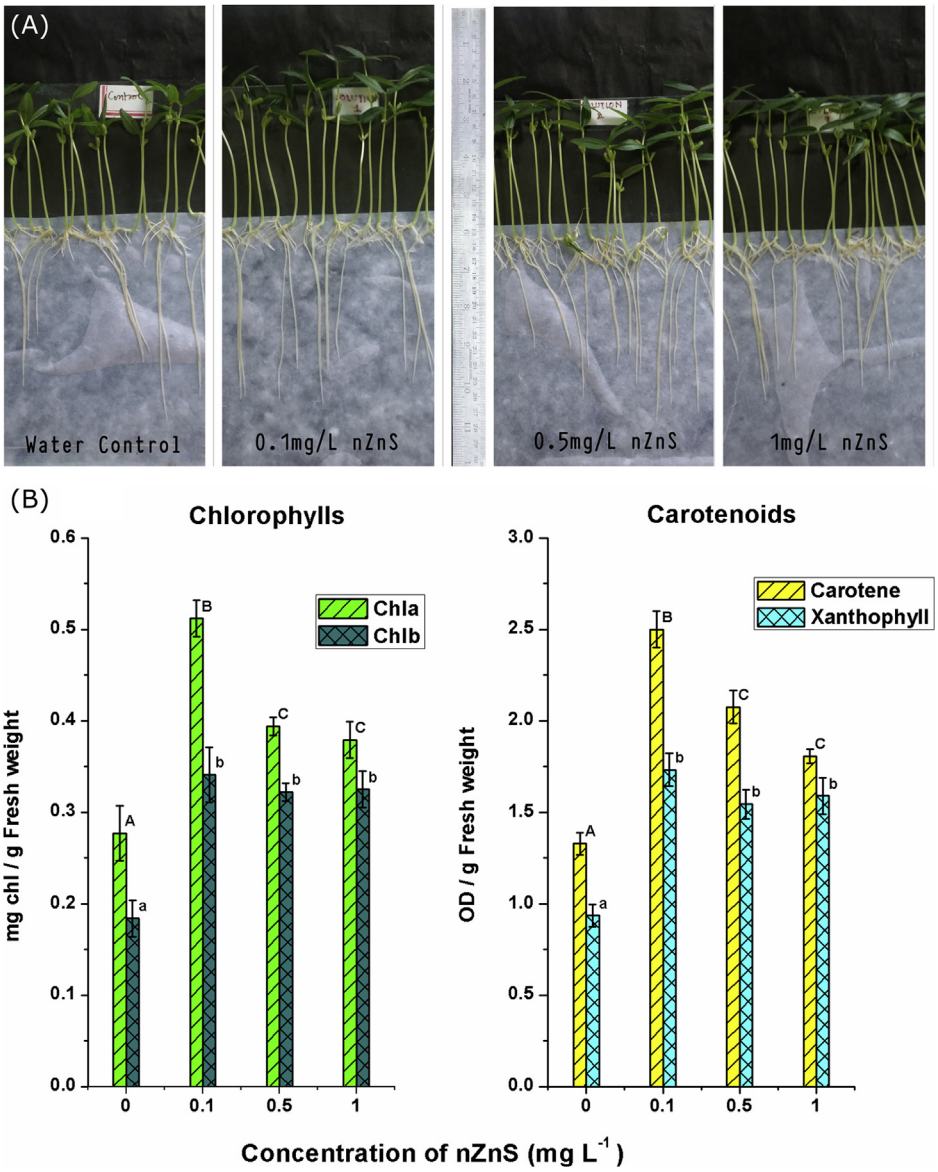

Fig. 2. (A) Morphology of control and nZnS treated plants after 10 days (B) Effect of nZnS on Chl a and Chl b, Carotene and xanthophyll content of 10 days treated mung bean plants. Different letters designate significant change at Tukey's test ($p < 0.05$). Values are means ± SE (n = 5).

The enzymatic oxidative product MDA was used as an index to measure the extent of membrane damage caused by ROS generation. Previously, Cabiscol Català et al. (2000), reported that ENPs can affect membrane integrity or permeability and lipid peroxidation by ROS generation. Interestingly, in our study, MDA content were significantly decreased in all the nZnS treatment concentrations than that recorded in the control plants (leaves; F = 43.751, $p \leq 0.001$ and roots; F = 68.642, $p \leq 0.001$, Fig. 3b). Results indicated that the nZnS application played a protective role in membrane integrity of plants, presumably due to its ability to induce the anti-stress enzymes (Pullagurala et al., 2018).

Proline is an important stress marker molecule, and plays a role in oxidative stress tolerance in plants. In our study, while no significant change was found in leaves, proline accumulation reduced significantly in the nZnS treated plant roots with respect to control (F = 5.067, $p \leq 0.012$, Fig. 3c). Sharma et al., (2012), have reported a decrease in MDA and proline content in *B. juncea* seedlings treated with AgNPs. They suggested that the declines in proline level indicate improved

Table 1
Effects of nZnS on root-shoot lengths, fresh-dry weights and rootlet numbers of 10 days treated mung bean plants. Values are mean ± SE (n = 5). Different letters designate significant change at Tukey's test ($p < 0.05$).

Treatments	Control	0.1 mg L^{-1} nZnS	0.5 mg L^{-1} nZnS	1 mg L^{-1} nZnS	F and p Values
Root length (cm)	7.1 ± 0.03 a	10.42 ± 0.23 b	9.79 ± 0.07 c	9.67 ± 0.19 c	F = 90.68, $p \leq 0.001$
Shoot length (cm)	10.2 ± 0.04 a	13.39 ± 0.05 b	12.71 ± 0.08 c	12.67 ± 0.07 c	F = 526.04, $p \leq 0.001$
Fresh weight (mg)	2.7 ± 0.02 a	4.54 ± 0.01 b	3.25 ± 0.03 c	2.95 ± 0.02 d	F = 1736.59, $p \leq 0.001$
Dry weight (mg)	0.2 ± 0.002 a	0.3 ± 0.001 b	0.27 ± 0.001 b	0.26 ± 0.001 b	F = 4.46, $p \leq 0.001$
Rootlet no.	8.2 ± 0.07 a	10.79 ± 0.01 b	10.48 ± 0.02 c	10.42 ± 0.01 c	F = 6804.95, $p \leq 0.001$

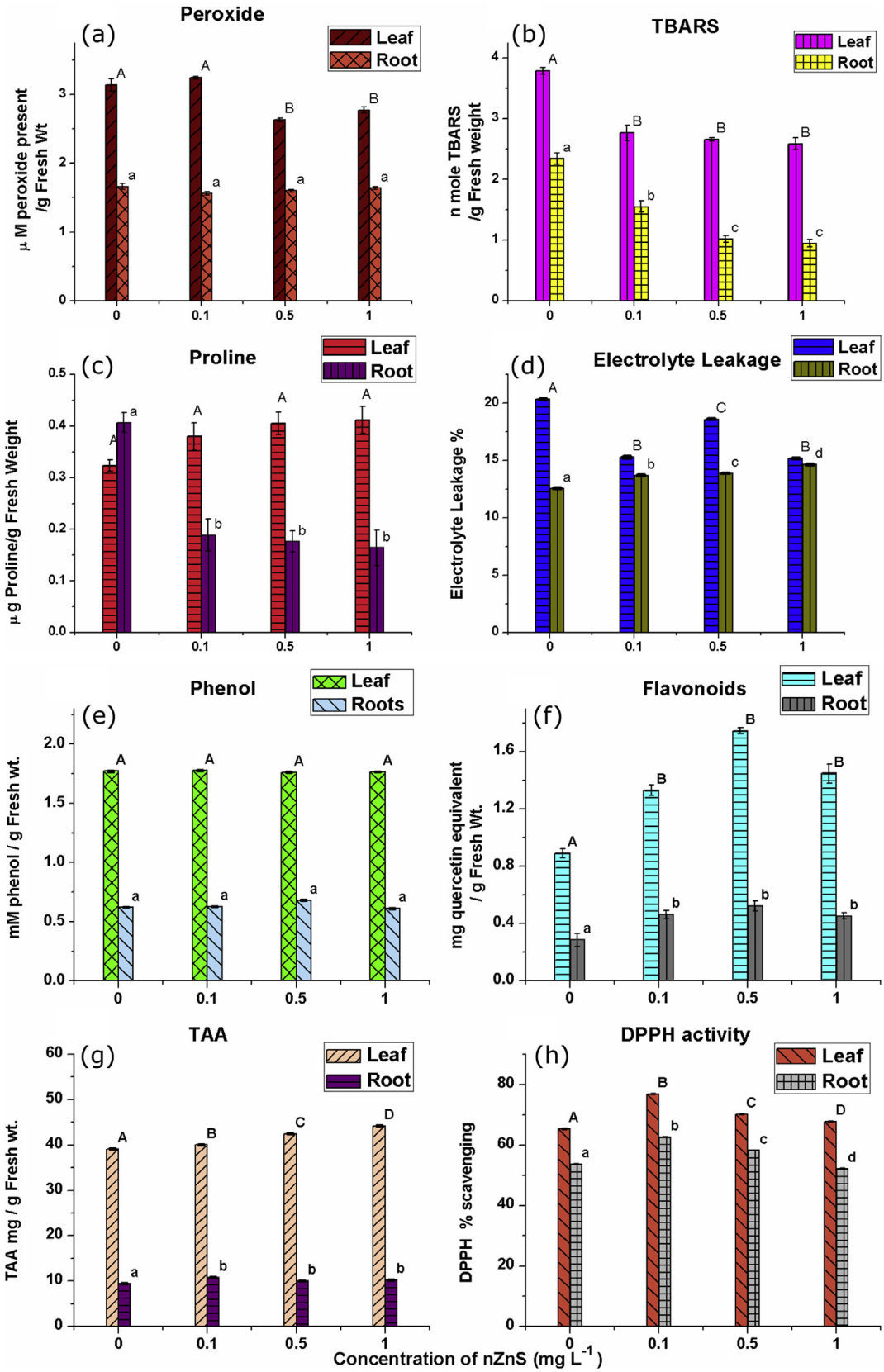

Fig. 3. (a) Peroxide contents (b) TBARS (c) Proline contents (d) Electrolyte leakage (e) Total phenol (f) Total flavonoid content (g) TAA and (h) DPPH activity of 10 days treated mungbean plants. Different letters designate significant changes at Tukey's test ($p < 0.05$). Values are means ± SE (n = 5).

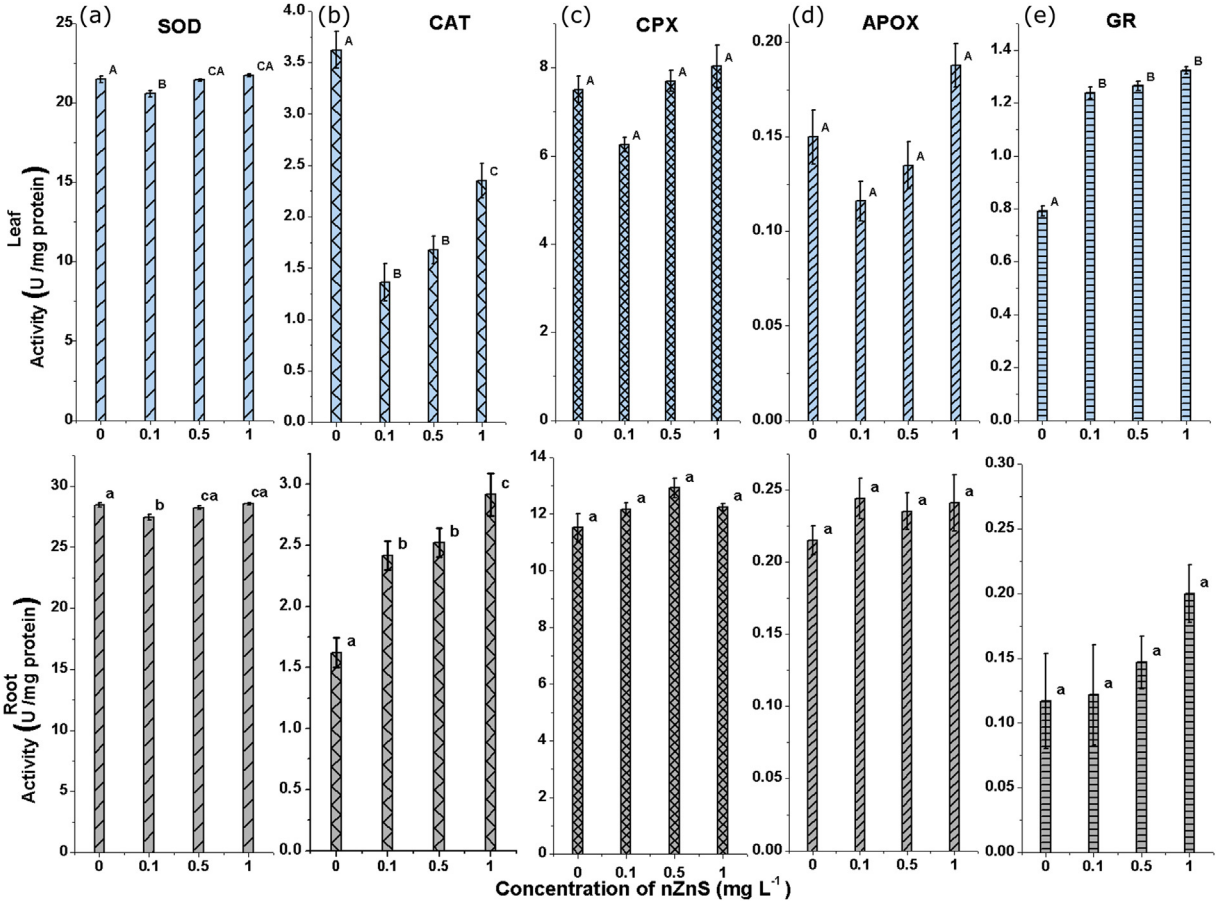

Fig. 4. Effects of nZnS treatments on enzymatic activities of (a) SOD (b) CAT (c) CPX (d) APOX and (e) GR. Values are means ± SE (n = 5). Different letters designate significant change at Tukey's test ($p < 0.05$).

electron exchange efficiency in the AgNPs treated seedlings. In line with Sharma et al, 2012, our result also showed enhanced pigment content and root-shoot growth might be due to improved electron exchange efficiency. Also, the reduction in lipid peroxidation by the application of the nZnS supports the proposed use of nZnS as a nanofertilizer in the future (Singh et al., 2013).

Electrolyte leakage is indicative of stress response in intact plant cells and is widely used as a measure of plant stress tolerance (Lutts et al., 1996). Conductivity measurements showed that nZnS treatment resulted in significant increase in root electrolyte leakage ($F = 9750.33$, $p \leq 0.001$, Fig. 3d). In roots ~9% increase in electrolyte leakage was observed at 0.1 mg L^{-1} nZnS concentration, 10% increase at 0.5 mg L^{-1} and 16% increase at 1 mg L^{-1}. These increased leakages could be the result of roots coming in the direct contact of the particles. When compared to previous studies, leakage observed in our study was not as dramatic as observed when plants were exposed to AgNPs (at 10 mg L^{-1}) and MWCNT (at 500 mg L^{-1}), which resulted in significant induction of ROS generation and oxidative stress (Oukarroum et al., 2012; De La Torre-Roche et al., 2013). Conversely, electrolyte leakage in leaves of treated seedlings were significantly reduced ($F = 3283.54$, $p \leq 0.001$). This result was in agreement with the reduction in MDA level indicating protective role of nZnS on membrane integrity (Pullagurala et al., 2018). Overall, nZnS treatments improved cellular electron exchange efficiency in treated seedlings (by maintaining optimum H_2O_2 concentration), arrested electron leakage, and by maintaining the ROS formation it could protect the cell membrane. No significant change in total protein content was observed in treated plants in comparison with the control [Supporting Information, Fig. S3].

3.2.4. Antioxidant defense system

Phenol and flavonoids are low molecular weight plant antioxidants which scavenge free radicals and protect antioxidant system (Ebrahimzadeh et al., 2010). In our study, no significant changes in phenol contents were observed in nZnS treated plants (Fig. 3e). However, flavonoid content was significantly increased in all the treated concentrations; the maximum increase was occurred at 0.5 mg L^{-1} treated leaf (leaves: $F = 14.91$, $p \leq 0.001$ and roots: $F = 9.27$, $p \leq 0.006$, Fig. 3f). Therefore, the increased flavonoids contents in the treated plants highlighted the antioxidant property of nZnS. Total antioxidant activity (TAA) in nZnS treated plants were also increased significantly than the control plants (leaves; $F = 1196.52$, $p \leq 0.001$ and Root; $F = 35.97$, $p \leq 0.001$, Fig. 3g). Similarly, increased DPPH scavenging activities were observed in treated plants (leaves; $F = 15615.83$, $p \leq 0.001$ and roots; $F = 10937.78$, $p \leq 0.001$, Fig. 3h). Plants showed a concentration dependent response in TAA, with increasing nZnS concentration TAA was also increased in treated leaves. On the other hand, highest DPPH activity was recorded at 0.1 mg L^{-1} nZnS concentration. Likewise, Abdel-Aziz et al, 2014, reported that AgNPs (5 mg L^{-1} to 20 mg L^{-1}) synthesized from *Chenopodium murale* leaf extract showed higher antioxidant and antimicrobial activity compared to *C. murale* leaf extract alone or silver nitrate. They showed that DPPH values increased in a dose dependent manner (Abdel-Aziz et al., 2014). Similarly, AgNPs synthesized from *Bergenia ciliata* showed higher TAA compared to the plant extract alone (Phull et al., 2016). Therefore, the results of our study demonstrated the antioxidant attributes of nZnS which would help in increasing the overall antioxidant capacity in mung bean plants.

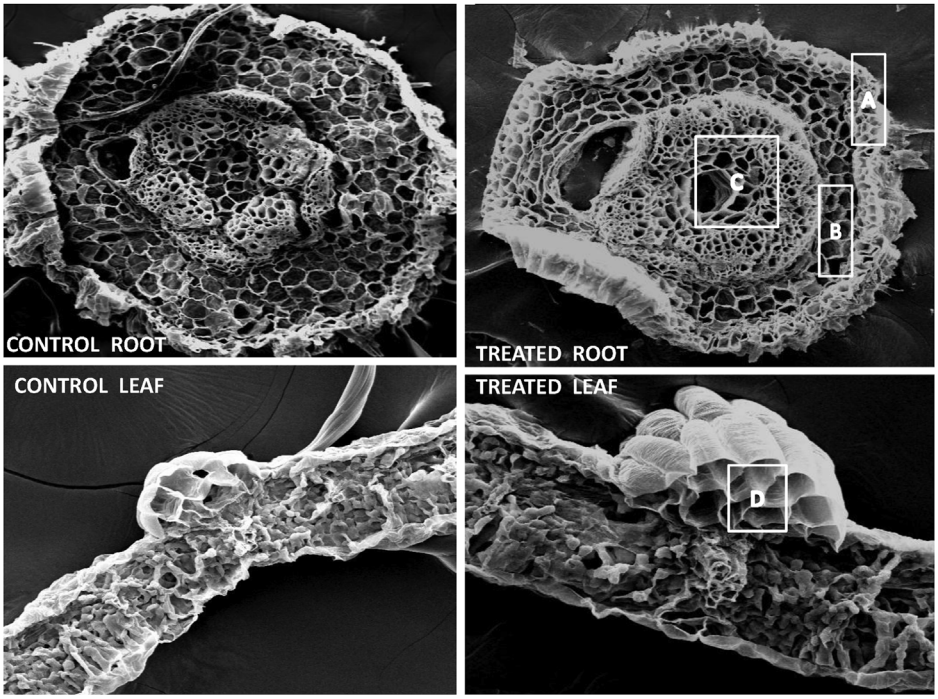

Fig. 5. Biological SEM image and EDX analysis of cross section from root tips and leaf of control plant and plant treated with 1 mg L^{-1} nZnS. (A) Epidermis, (B) Parenchyma (C) Vascular cylinder (D) Leaf midrib.

3.2.5. nZnS treated plants did not trigger oxidative stress

To test the effects of nZnS on ROS generation and oxidative stress in mung bean plants, activities of superoxide dismutase (SOD), catalase (CAT), catechol peroxidase (CPX), ascorbate (APOX) and glutathione (GR) were measured.

SOD is a powerful stress enzyme that catalyzes the dismutation of O_2^- to H_2O_2. In the present study, change in SOD activity was found only at 0.1 mg L^{-1} nZnS concentration, where significantly decreased activity was recorded in both roots and leaves (3.5% and 4.2% respectively), indicating the protective role of nZnS against oxidative stress (leaves; $F = 9.51$, $p \leq 0.005$ and roots; $F = 8.77$, $p \leq 0.007$, Fig. 4a). The decreased SOD activity recorded here might be the result of antioxidant activity of nZnS.

In comparison to control, marked increased in root CAT activities (49% for 0.1 mg L^{-1}, 55.39% for 0.5 mg L^{-1} and 79.73% for 1 mg L^{-1} nZnS) were recorded in nZnS treated plants ($F = 240.99$, $p \leq 0.001$), whereas, activities in leaves decreased (62.46% for 0.1 mg L^{-1}, 54% for 0.5 mg L^{-1} and 35.08% for 1 mg L^{-1} nZnS; $F = 95.553$, $p \leq 0.001$, Fig. 4b). The enhanced root CAT activities, corresponded with the low levels of electrolyte leakage observed in nZnS treated roots, confirmed that the primary organs which come in contact with the ENPs changed CAT activity that might vary according to the intensity of stress, time of treatment and induction of new isozymes. The plausible reason for the decreased CAT activities in leaves might be due to the existence of certain level of ROS production even in the control seedlings. Thus the regulation of catalase activity must occur by a specific mechanism, not by peroxisomal turnover (Chance and Maehly, 1955).

However, no alteration in the CPX activities were observed in nZnS treated mung bean plants (Fig. 4c), a similar trend observed in H_2O_2 generation, and was in agreement with the commonly observed positive correlation between the antioxidant enzymes and stress levels in plants. The APOX is known to have higher affinity towards H_2O_2 than CAT. It is an enzyme in the Halliwell-Asada pathway (ascorbate – glutathione cycle), a network of oxidation-reduction reactions that directly reduces the H_2O_2 generated by SOD into H_2O (Supporting Fig. S5). Besides, ascorbate peroxidase (APOX) readily dismutes H_2O_2 using ascorbate as the electron donor (Foyer and Halliwell, 1976). As shown in Fig. 4d, no significant changes in APOX activities were recorded in both leaves and roots of the treated plants. These results clearly indicated that peroxidase, lipid peroxidation and APOX enzymes activities synergistically corroborated with each other and nZnS treatments did not induce any kind of oxidative stress and maintained cellular homeostasis.

Glutathione reductase (GR) catalyzes the generation of reduced glutathione (GSH) via Halliwell-Asada pathway, needed for the regeneration of ascorbate (Supporting Fig. S5) (Foyer and Halliwell, 1976). A significant ($F = 219.49$, $p \leq 0.001$) increase in GR activities were found in the leaves of nZnS treated seedlings (56.44% for 0.1 mg L^{-1}, 59.6% for 0.5 mg L^{-1} and 67.05% for 1 mg L^{-1} nZnS), however no change was observed in the roots (Fig. 4e). Considering that no alteration in APOX activates were recorded, this increase in GSH activities in leaves might be the result of sulfur supplementation via nZnS treatments (Nayan et al., 2016). Previously, Xiang et al, 2001, reported that plants with decreased GR activities were smaller in size and are more sensitive to environmental stresses (Xiang et al., 2001). May et al. (1998), also demonstrated that increased levels of reduced glutathione provided plants with selective advantage to overcome suboptimal growth conditions. Therefore, the increased shoot lengths observed in the treated plants might be the result of increased GR activities. Thus, the results showed that optimum concentration of nZnS triggered improved growth and adaptability in mung bean plants via increased GR activity.

3.3. Uptake and translocation of nZnS, and its effects on plant cell microstructure

3.3.1. Microscopic evidence of uptake, transport and accumulation of nZnS

nZnS/ionic Zn distribution pattern in cross sections of control and treated plants roots and leaves were obtained using SEM with EDX. SEM images revealed low concentrations of Zn in roots and leaves tissues of treated plants (Fig. 5), whereas no Zn was found in control plants. The presence of low concentration of Zn in treated plants suggested possible internalization of nZnS into the plants (Du et al., 2015). In roots, Zn was observed in epidermis, parenchyma, but was not detected in the vascular cylinder which indicated that most of the applied nZnS entered

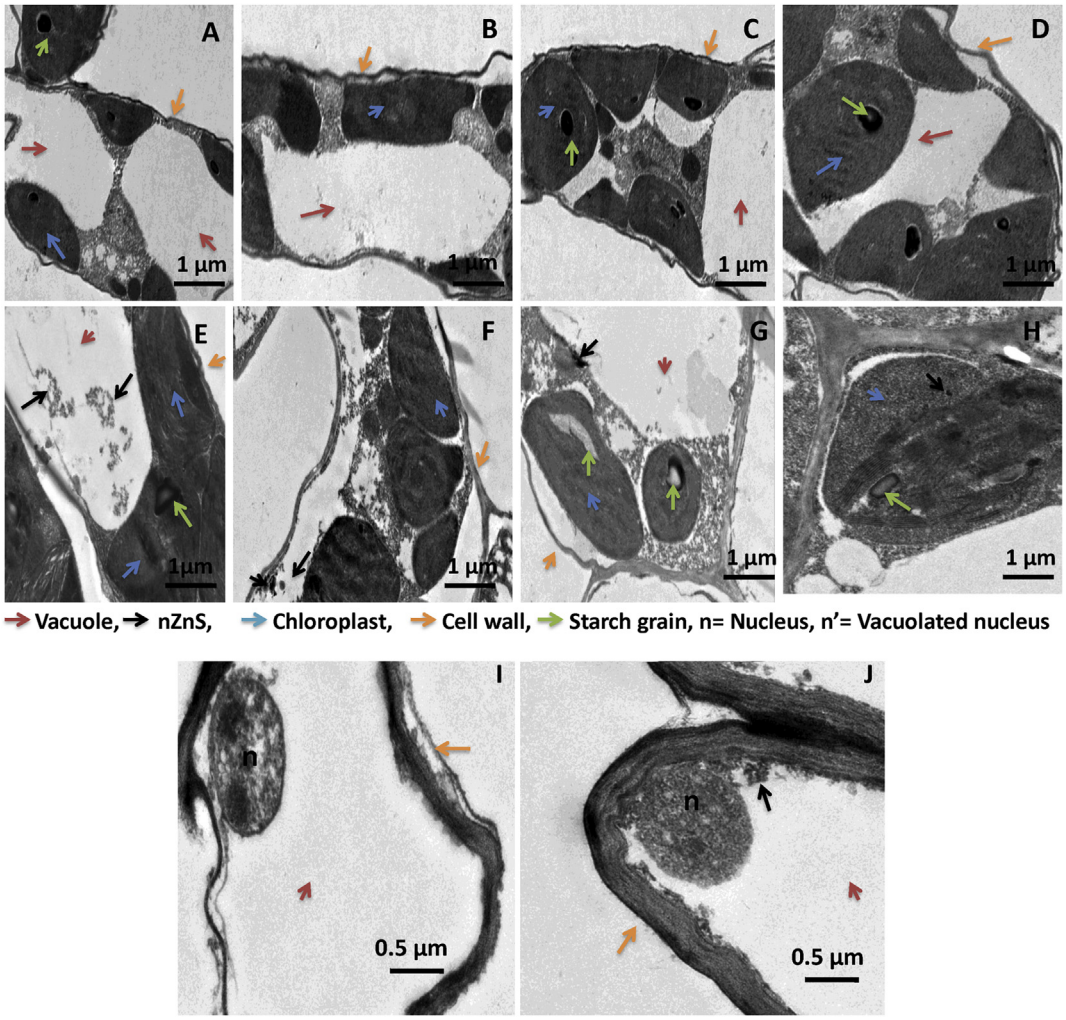

Fig. 6. TEM images of mung bean plant; leaves (control: A, B, C, D and treated with nZnS: E, F, G, H) and roots (control: I and treated with nZnS: J).

into the root cells and accumulated in the parenchyma region [Supporting Tables S1–S5]. Similar result was found by Du et al., (2015), who exposed wheat plants to nCeO at 100 and 400 mg kg^{-1}. TEM images further confirmed this information, where nZnS were observed to be present primarily in the vacuoles of the parenchyma cells. Weight percentage of elements and EDX analysis were presented in Supporting Information [Supporting Tables S1–S5].

As seen in Fig. 5, neither roots nor the leaf tissues of the treated plants showed any structural aberrations and membrane damage. Applications of ENPs often cause structural aberration in plants. For example, Lin and Xing (2008), reported that exposure of nZnO in ryegrass caused shrunk root tips and highly vacuolated root cells. Wang et al. (2011), also showed that ultra-small anatase, $nTiO_2$ caused dysfunction of microtubules and tubulin monomers in *A. thaliana*. In contrast, nZnS treatment did not generate such phytotoxic responses, while Zn was detected by EDX analysis [Supporting Tables S1–S5] in leaf midrib proving that nZnS/ionic Zn reached the transport system and was acropetally translocated from root to leaf. TEM images of treated leaf sections showed accumulation of nZnS in vacuoles and chloroplast regions (Fig. 6E–H). However, control plants were devoid of ENPs or aggregates (Fig. 6A–D). In treated plant's root section, ENPs were mainly accumulated in the vacuoles (Fig. 6J), whereas in control plants no such dark particles were observed in roots (Fig. 6I). According to reported studies, particles up to 20 nm were taken up by plant cells through plasmodesmata and endocytosis (Dietz and Herth, 2011). For example, Lin and Xing (2008), used TEM to show that nZnO passed through the epidermis and cortex of roots of *Lolium perenne* L. (ryegrass), but they did not examine if they are present within the shoots. Zhu et al. (2008) used magnetization to show the uptake and subsequent transport of magnetite nFe_3O_4 by *Cucurbita maxima* (pumpkin) grown in solution culture. However, no nFe_3O_4 (i.e., magnetic signals) were detected in shoots of soil cultured plants. Also, Navarro et al. (2012), used polymer coated CdS/ZnS QDs to show uptake by *A. thaliana* but no internalization and translocation as intact QDs occurred after 7 days of exposure. But in our study, microscopic images evidenced that nZnS could penetrate the root cell wall and translocate acropetally via the water transport system to the leaves without altering cell structures. The uptake of ENPs by the plants is dependent on many factors; the stability of ENPs in the suspension is one of the important reasons among them. Thus, from environmental point of view investigations on the long term stability of ENPs in different systems and in soil are important.

3.3.2. Zn release from nZnS

In vitro ICPMS at pH 7.0 studies on release of Zn from treatment concentrations (0.1, 0.5 and 1 mg L^{-1}) of nZnS, revealed that very small amounts of 0.001 ppm, 0.003 ppm, and 0.005 ppm Zn were released, respectively, after 24 h. *In vivo* study of distribution of nZnS on plant samples was also studied using ICPMS. Results showed that nZnS treated plant samples had small but significant concentration dependent enhancements in Zn contents in both roots ($F = 50.460$, $p < 0.001$) and leaves ($F = 104.998$, $p < 0.001$) with respect to

control [Supporting Fig. S4]. Results also confirmed the slow release of Zn from nZnS and its uptake by treated plants. The highest concentration of Zn was accumulated in roots than leaves of treated plants due to the direct exposure to the treatment solutions. Also, the dose dependent increase of Zn in treated plant leaves compared to control confirmed the translocation of nZnS from root to leaves.

3.3.3. Potential for nZnS to be use as a micronutrient

As revealed by the TEM images, presence of nZnS aggregates, mostly in vacuoles, suggested that nZnS moved from xylem's sap to aerial tissues with apoplastic flow (through cell wall) and symplastic transport (through cytoplasm). Further studies will be required to validate this finding. Also, the low biomass distribution of Zn in the tissues indicated the low dissolution rate of nZnS, which remained in nano form after 10 days of treatment. The particles which were found in TEM analysis primarily had a diameter of 20 ± 0.2 nm. However, the average size of the applied particles was 13.3 ± 0.3 nm. This could be explained by the fact that nZnS formed agglomerates in the cell medium, which were slightly larger than the initial particle sizes. The released Zn together with nZnS was carried through to the leaf of the plant samples interacted with microenvironment of treated plant cells and augmented pigment level and plant growth, in contrast with the control. Therefore, nZnS application has the potential to correct Zn level in crops. Again, photosynthesis is a well established source of ROS in plants. Superoxide and H_2O_2 are generated by photosynthetic components on Photosystem I (PSI). A balance must be maintained between ROS generation and scavenging in plant system. Importance of the antioxidants in maintaining photosynthesis has been reported earlier by many researchers (for example, see Pradhan et al., 2013). In this context, our study demonstrated that the applied nZnS positively altered plant growth performance and antioxidant status. Increased chlorophyll content, the optimum level of H_2O_2 and superoxide molecules, and enhanced antioxidant capacity in nZnS treated plants highlighted the nZnS antioxidant machinery that might act in PSI and regulate cyclic electron flow to limit singlet oxygen production at PhotosystemII (PSII). Also, the significant reduction in lipid peroxidation by nZnS treatment favours the proposed use of nZnS as a nanofertilizer in the future and a detail mechanistic study on reason behind this will be interesting. Again, high antioxidant capacity in nZnS treated plants is beneficial because it desensitizes photosynthesis to overreduction in the Photosynthetic Electron Transport chain. Thus present study demonstrated the potential beneficial role of nZnS in altering metabolic pathways of mung bean plant but a life cycle study is also necessary.

4. Conclusion

Our study evidenced that nZnS treatments promoted root-shoot lengths and produced higher photosynthetic pigments in treated plants. The biochemical assays conducted during the study evidenced that among the tested doses of nZnS, 0.1 mg L^{-1} was optimal for inducing maximal growth stimulatory responses. None of the treatments triggered any oxidative stress but improved antioxidant system of the treated mung bean plants. The electron microscope studies confirmed uptake and translocation of nZnS in treated plants and also showed that it did not cause any damage to the cellular microstructure. Therefore, given the growth promotion effects of nZnS treatment in plants, it can be concluding that it has the potential to be used as a micronutrient for plant growth and photosynthetic enhancements in plants. While further studies will be necessary before nZnS could be recommended for field use, the results generated in our study provided preliminary information about the novel plant-modulatory roles of nZnS nanoparticle.

Conflicts of interest

There are no conflicts to declare.

Author contribution

Each author contributed significantly in the manuscript. The addresses of the authors are given in the manuscript.

Acknowledgements

We are thankful to Indian Statistical Institute, Kolkata for providing financial support. We also acknowledge Mr. Sandipan Chakraborty at Reprocell India for his help.

Appendix A. Supplementary data

Supplementary data to this article can be found online at https://doi.org/10.1016/j.plaphy.2019.06.031.

References

Abdel-Aziz, M.S., et al., 2014. Antioxidant and antibacterial activity of silver nanoparticles biosynthesized using *Chenopodium murale* leaf extract. J. Saudi Chem. Soc. 18 (4), 356–363.
Alhakmani, F., Kumar, S., Khan, S.A., 2013. Estimation of total phenolic content, in–vitro antioxidant and anti–inflammatory activity of flowers of *Moringa oleifera*. Asian Pac. J. Trop. Biomed. 3 (8), 623–627.
Almutairi, Z.M., 2016. Effect of nano-silicon application on the expression of salt tolerance genes in germinating tomato (*Solanum lycopersicum* L.) seedlings under salt stress. Plant Omics 9 (1), 106.
Arnon, D.I., 1949. Copper enzymes in isolated chloroplasts. Polyphenoloxidase in *Beta vulgaris*. Plant Physiol. 24 (1), 1.
Asli, S., Neumann, P.M., 2009. Colloidal suspensions of clay or titanium dioxide nanoparticles can inhibit leaf growth and transpiration via physical effects on root water transport. Plant Cell Environ. 32 (5), 577–584.
Awasthi, A., et al., 2017. Effect of ZnO nanoparticles on germination of *Triticum aestivum* seeds. In: Macromolecular Symposia. Wiley Online Library.
Bates, L., Waldren, R., Teare, I., 1973. Rapid determination of free proline for water-stress studies. Plant Soil 39 (1), 205–207.
Berube, D.M., et al., 2010. Project on emerging nanotechnologies-consumer product inventory evaluated. Nanotech. L. & Bus. 7, 152.
Bhattacharjee, B., Chatterjee, N., Lu, C.-H., 2013. Harmful Impact of ZnS Nanoparticles on *Daphnia Sp*. In the Western Part (Districts of Bankura and Purulia) of West Bengal. ISRN Nanomaterials, India 2013.
Blois, M.S., 1958. Antioxidant determinations by the use of a stable free radical. Nature 181 (4617), 1199.
Cabiscol Català, E., Tamarit Sumalla, J., Ros Salvador, J., 2000. Oxidative stress in bacteria and protein damage by reactive oxygen species. Int. Microbiol. 3 (1), 3–8 2000.
Chance, B., Maehly, A., 1955. [136] Assay of Catalases and Peroxidases.
Davis, A.R., Fish, W.W., Perkins-Veazie, P., 2003. A rapid spectrophotometric method for analyzing lycopene content in tomato and tomato products. Postharvest Biol. Technol. 28 (3), 425–430.
De La Torre-Roche, R., et al., 2013. Multiwalled carbon nanotubes and C_{60} fullerenes differentially impact the accumulation of weathered pesticides in four agricultural plants. Environ. Sci. Technol. 47 (21), 12539–12547.
Dietz, K.J., Herth, S., 2011. Plant nanotoxicology. Trends Plant Sci. 16 (11), 582–589.
Du, W., et al., 2015. Physiological and biochemical changes imposed by CeO_2 nanoparticles on wheat: a life cycle field study. Environ. Sci. Technol. 49 (19), 11884–11893.
Ebrahimzadeh, M.A., et al., 2010. Antioxidant activity of the bulb and aerial parts of *Ornithogalum sintenisii* L (Liliaceae) at flowering stage. Trop. J. Pharmaceut. Res. 9 (2).
Fang, X., et al., 2011. ZnS nanostructures: from synthesis to applications. Prog. Mater. Sci. 56 (2), 175–287.
Foyer, C.H., Halliwell, B., 1976. The presence of glutathione and glutathione reductase in chloroplasts: a proposed role in ascorbic acid metabolism. Planta 133 (1), 21–25.
Fu, Y.Q., et al., 2012. Delivering DNA into plant cell by gene carriers of ZnS nanoparticles. Chem. Res. Chin. Univ. 28 (4), 672–676.
Ghafariyan, M.H., et al., 2013. Effects of magnetite nanoparticles on soybean chlorophyll. Environ. Sci. Technol. 47 (18), 10645–10652.
Giannopolitis, C.N., Ries, S.K., 1977. Superoxide dismutases: I. Occurrence in higher plants. Plant Physiol. 59 (2), 309–314.
Hodges, D.M., et al., 1999. Improving the thiobarbituric acid-reactive-substances assay for estimating lipid peroxidation in plant tissues containing anthocyanin and other interfering compounds. Planta 207 (4), 604–611.
Huang, F.H., Peng, Y.R., Lin, C.F., 2006. Synthesis and characterization of ZnS: Ag nanocrystals surface-capped with thiourea. Chem. Res. Chin. Univ. 22 (6), 675–678.
Jin, Q., et al., 2016. The "off–on" phosphorescent switch of Mn-doped ZnS quantum dots for detection of glutathione in food, wine, and biological samples. Sensor. Actuator. B Chem. 227, 108–116.
Karthikeyan, B., et al., 2016. Role of ZnS nanoparticles on endoplasmic reticulum stress-mediated apoptosis in retinal pigment epithelial cells. Biol. Trace Elem. Res. 170 (2), 390–400.

LIN, Q., 2005. Subcellular localization of copper in tolerant and non-tolerant plant. J. Environ. Sci. 17 (3), 452–456.
Lin, D., Xing, B., 2008. Root uptake and phytotoxicity of ZnO nanoparticles. Environ. Sci. Technol. 42 (15), 5580–5585.
López, M.L., et al., 2017. Effect of ZnO nanoparticles on corn seedlings at different temperatures; X-ray absorption spectroscopy and ICP/OES studies. Microchem. J. 134, 54–61.
Lowry, O.H., et al., 1951. Protein measurement with the Folin phenol reagent. J. Biol. Chem. 193 (1), 265–275.
Lutts, S., Kinet, J., Bouharmont, J., 1996. NaCl-induced senescence in leaves of rice (*Oryza sativa* L.) cultivars differing in salinity resistance. Ann. Bot. 78 (3), 389–398.
Mahajan, P., Dhoke, S., Khanna, A., 2011. Effect of nano-ZnO particle suspension on growth of mung (*Vigna radiata*) and gram (*Cicer arietinum*) seedlings using plant agar method. J. Nanotechnol. 2011, 1–7.
May, M.J., et al., 1998. Glutathione homeostasis in plants: implications for environmental sensing and plant development. J. Exp. Bot. 49 (321), 649–667.
Mukherjee, A., et al., 2014. Physiological effects of nanoparticulate ZnO in green peas (*Pisum sativum* L.) cultivated in soil. Metallomics 6 (1), 132–138.
Nakano, Y., Asada, K., 1981. Hydrogen peroxide is scavenged by ascorbate-specific peroxidase in spinach chloroplasts. Plant Cell Physiol. 22 (5), 867–880.
Navarro, D.A., Bisson, M.A., Aga, D.S., 2012. Investigating uptake of water-dispersible CdSe/ZnS quantum dot nanoparticles by *Arabidopsis thaliana* plants. J. Hazard Mater. 211, 427–435.
Nayan, R., et al., 2016. Zinc sulfide nanoparticle mediated alterations in growth and antioxidant status of *Brassica juncea*. Biologia 71 (8), 896–902.
Oukarroum, A., et al., 2012. Inhibitory effects of silver nanoparticles in two green algae, *Chlorella vulgaris* and *Dunaliella tertiolecta*. Ecotoxicol. Environ. Saf. 78, 80–85.
Pathak, C., Mandal, M., Agarwala, V., 2013. Synthesis and characterization of zinc sulphide nanoparticles prepared by mechanochemical route. Superlattice. Microst. 58, 135–143.
Pathakoti, K., et al., 2013. In vitro cytotoxicity of CdSe/ZnS quantum dots with different surface coatings to human keratinocytes HaCaT cells. J. Environ. Sci. 25 (1), 163–171.
Phull, A.R., et al., 2016. Antioxidant, cytotoxic and antimicrobial activities of green synthesized silver nanoparticles from crude extract of *Bergenia ciliata*. Future J. Pharmaceut. Sci. 2 (1), 31–36.
Pradhan, S., et al., 2013. Photochemical modulation of biosafe manganese nanoparticles on *Vigna radiata*: a detailed molecular, biochemical, and biophysical study. Environ. Sci. Technol. 47 (22), 13122–13131.
Prieto, P., Pineda, M., Aguilar, M., 1999. Spectrophotometric quantitation of antioxidant capacity through the formation of a phosphomolybdenum complex: specific application to the determination of vitamin E. Anal. Biochem. 269 (2), 337–341.
Pullagurala, V.L.R., et al., 2018. ZnO nanoparticles increase photosynthetic pigments and decrease lipid peroxidation in soil grown cilantro (*Coriandrum sativum*). Plant Physiol. Biochem. 132, 120–127.
Rawat, S., et al., 2019. Differential physiological and biochemical impacts of nano vs micron Cu at two phenological growth stages in bell pepper (*Capsicum annuum*) plant. NanoImpact 14, 100161.
Rico, C.M., et al., 2013. Effect of cerium oxide nanoparticles on rice: a study involving the antioxidant defense system and in vivo fluorescence imaging. Environ. Sci. Technol. 47 (11), 5635–5642.
Saha, P., Kunda, P., Biswas, A.K., 2012. Influence of sodium chloride on the regulation of Krebs cycle intermediates and enzymes of respiratory chain in mungbean (*Vigna radiata* L. Wilczek) seedlings. Plant Physiol. Biochem. 60, 214–222.
Santos, A.R., et al., 2010. The impact of CdSe/ZnS quantum dots in cells of *Medicago sativa* in suspension culture. J. Nanobiotechnol. 8 (1), 24.
Sharma, P., et al., 2012. Silver nanoparticle-mediated enhancement in growth and antioxidant status of *Brassica juncea*. Appl. Biochem. Biotechnol. 167 (8), 2225–2233.
Siddiqui, M.H., Al-Whaibi, M.H., 2014. Role of nano-SiO2 in germination of tomato (*Lycopersicum esculentum* seeds Mill.). Saudi J. Biol. Sci. 21 (1), 13–17.
Singh, N., et al., 2013. Zinc oxide nanoparticles as fertilizer for the germination, growth and metabolism of vegetable crops. J. Nanoeng. Nanomanuf. 3 (4), 353–364.
Sinha, A.K., 1972. Colorimetric assay of catalase. Anal. Biochem. 47 (2), 389–394.
Slomberg, D.L., Schoenfisch, M.H., 2012. Silica nanoparticle phytotoxicity to *Arabidopsis thaliana*. Environ. Sci. Technol. 46 (18), 10247–10254.
Suriyaprabha, R., et al., 2012. Silica nanoparticles for increased silica availability in maize (*Zea mays*. L) seeds under hydroponic conditions. Curr. Nanosci. 8 (6), 902–908.
Suyana, P., et al., 2014. Antifungal properties of nanosized ZnS particles synthesised by sonochemical precipitation. RSC Adv. 4 (17), 8439–8445.
Thurman, R.G., Ley, H.G., Scholz, R., 1972. Hepatic microsomal ethanol oxidation: hydrogen peroxide formation and the role of catalase. Eur. J. Biochem. 25 (3), 420–430.
Wang, S., Kurepa, J., Smalle, J.A., 2011. Ultra-small TiO_2 nanoparticles disrupt microtubular networks in *Arabidopsis thaliana*. Plant Cell Environ. 34 (5), 811–820.
Wang, Z., et al., 2016. CuO nanoparticle interaction with *Arabidopsis thaliana*: toxicity, parent-progeny transfer, and gene expression. Environ. Sci. Technol. 50 (11), 6008–6016.
Womack, F.N., et al., 2004. Measurement of triboluminescence and proton half brightness dose for ZnS: Mn. IEEE Trans. Nucl. Sci. 51 (4), 1737–1741.
Xiang, C., et al., 2001. The biological functions of glutathione revisited in *Arabidopsis* transgenic plants with altered glutathione levels. Plant Physiol. 126 (2), 564–574.
Yang, Y., et al., 2014. Toxicity and biodistribution of aqueous synthesized ZnS and ZnO quantum dots in mice. Nanotoxicology 8 (1), 107–116.
Żaba, A., et al., 2016. Zinc Sulphide (ZnS) Nanparticles for Advanced Application. Czasopismo Techniczne, pp. 125–134 2016 (Chemia Zeszyt 1 Ch (4) 2016.
Zhang, P., Ma, Y., Zhang, Z., 2015. Interactions between engineered nanomaterials and plants: phytotoxicity, uptake, translocation, and biotransformation. In: Nanotechnology and Plant Sciences. Springer, pp. 77–99.
Zhu, H., et al., 2008. Uptake, translocation, and accumulation of manufactured iron oxide nanoparticles by pumpkin plants. J. Environ. Monit. 10 (6), 713–717.